

# Spin-imbalanced topological phases and chiral Rashba states in a fermionic lattice

N. Goldman\*

*Center for Nonlinear Phenomena and Complex Systems - Université Libre de Bruxelles (U.L.B.), B-1050 Brussels, Belgium*

W. Beugeling and C. Morais Smith

*Institute for Theoretical Physics, Utrecht University,  
Leuvenlaan 4, 3584 CE Utrecht, the Netherlands*

**The quantum Hall effect – the exact quantization of the transverse Hall conductivity– finds its roots in time-reversal symmetry breaking perturbations. Indeed, a magnetic field can produce chiral edge states, which transport current without dissipation. Recently, the realm of quantum Hall physics has revealed novel quantum phases, with the discovery of the quantum spin Hall effect. The latter was observed in materials with important spin-orbit interactions and leads to finite spin-conductivity. This intrinsic spin-orbit interaction acts as equal but opposite magnetic fields on each spin component and produces counter-propagating edge states with opposite spins. Here we reveal new topological phases that arise when the effects produced by spin-orbit couplings and magnetic fields are combined. We demonstrate that this system provides an elegant setup to generate rich and robust spin-structures propagating along the edge of a sample. The exquisite control over these polarized current-carrying states will pave an interesting route for the development of quantum spintronics.**

## I. INTRODUCTION

The discovery of the first topological state of matter – the integer quantum Hall (QH) effect – has revolutionized our understanding of condensed matter<sup>1</sup>. For the first time, we were confronted with a material that had different bulk and edge properties. Indeed, a gas of electrons in two dimensions subjected to a perpendicular magnetic field is gapped and insulating in the bulk, but is metallic at the edges, which carry quantized charge currents without dissipation. The charge carriers (electrons) have an internal “spin” angular momentum, which can point up or down. In the QH effect, two currents on the same edge, one for spin up, another for spin down, move in the same direction – they are chiral – and transport charge without transporting spin. The quantization of the transverse (Hall) conductance  $\sigma_H = \nu(e^2/h)$  is directly related to the number of these chiral edge states  $\nu$ , which is a sum of topologically protected Chern numbers<sup>2,3</sup>.

The proposal by Kane and Mele<sup>4,5</sup> that a new topological state of matter could be realized in graphene by taking into account spin-orbit interactions has brought about the quantum spin Hall (QSH) effect, in which the edge

currents carry spin but no charge. This spin-transport is realized by helical edge states, namely spins traveling in opposite directions along the edge (cf. Fig. 1 (b)), and is protected by a  $\mathbb{Z}_2$  topological index<sup>4,5</sup>. Contrarily to the integer QH effect, which is rooted in a time-reversal symmetry breaking perturbation (i.e., the magnetic field), the QSH effect occurs in systems where this symmetry is preserved. The spin-orbit coupling links the spin of an electron to its linear momentum  $\mathbf{p} = \hbar\mathbf{k}$ . The coupling may be intrinsic to a material, the so-called intrinsic spin-orbit (ISO) interaction, or may be generated by external fields that break the inversion symmetry of the graphene lattice, such as the Rashba or the Dresselhaus spin-orbit interactions. In a tight-binding description, the ISO term corresponds to a next-nearest-neighbor (NNN) hopping under the effect of the  $\hat{\sigma}_z$  Pauli matrix, which attributes opposite signs for spin up and spin down hopping electrons, but keeps the spin along one specific ( $z$ ) direction. On the other hand, the Rashba term has the form of a nearest-neighbor (NN) hopping which only couples NNs with opposite spin. This term tends to misalign the spin by rotating it towards the plane of the sample. The ISO interaction opens a gap in the spectrum but preserves the spin degeneracy of the energy bands, whereas the Rashba term does the opposite.

The two topological states of matter described above produce either charge or spin edge currents that are dissipation-free and robust against disorder, due to their topological character. An interesting question is whether more involved situations could occur: could it be possible to transport both quantized spin and charge simultaneously? Furthermore, would it be possible to manipulate the spin of the quantized edge currents and rotate them at will, thus generating richer spin structures than in standard topological insulating phases?

In this paper, we show that a magnetic field applied perpendicularly to a two-dimensional (2D) lattice, combined with the intrinsic and Rashba spin-orbit terms, may lead to novel and interesting effects, not considered so far. The perpendicular magnetic field generates a gauge field that influences all the hopping terms (i.e., the usual hopping, the Rashba, and the ISO terms), but also a Zeeman splitting, which filters the spins. Different combinations of these terms will provide us with unexpected topological states of matter, such as a spin-imbalanced topological phase and complex chiral spin textures.

The observation of the novel phases discussed here may have profound implications for spintronics.

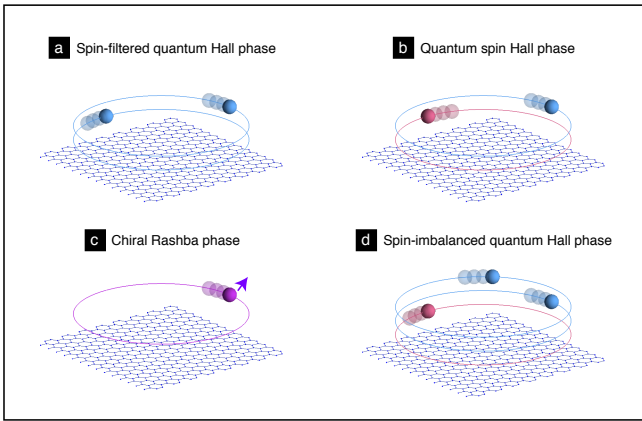


FIG. 1: **Spin-textures and quantum Hall phases:** Spin-up and spin-down components are represented by blue and red balls, respectively. (a) The spin-filtered quantum Hall phase: the chiral edge states are constituted of identical spins with same orientation. (b) The QSH phase: the helical edge states are formed by counter-propagating spins of opposite sign. (c) The Chiral Rashba phase: a single chiral edge state is formed with arbitrary spin direction, represented in purple. (d) The spin-imbalanced QH phase: the chiral edge states feature several spins of different nature such that  $N_{\uparrow} \neq N_{\downarrow}$ .

Spin-polarized injection in a ferromagnet-semimetal-ferromagnet heterojunction is at the heart of the Datta-Das transistor<sup>6</sup>, where the propagation or blocking of the current depends on whether the semimetal between the spin-up and spin-down ferromagnets allows or not for a rotation of the spin. Our results indicate that by tuning the external electric field, and hence the Rashba term, the on-off regimes may be selected in the quantum regime. In addition, chiral spin-imbalanced 1D edge states represent the realization of tiny devices, where both types of spin may be transported, but in different and controllable proportions. The recently discovered mercury- and bismuth-telluride compounds, which exhibit the QSH effect due to large spin-orbit coupling, are realistic candidates for the observation of the quantum spin-imbalance effect unveiled here.

### A. The model

We consider a model of spin-1/2 fermions in a honeycomb lattice subjected to a uniform perpendicular magnetic field  $\mathbf{B} = B\mathbf{1}_z$ . The presence of the magnetic field modifies the spin-1/2 graphene model of Refs. 4,5 in two fundamentally different manners. First, the magnetic field acts on the charges through the minimal coupling  $\mathbf{p} - e\mathbf{A}$ , where  $\mathbf{A}$  is the gauge potential, and enters the model through the so-called Peierls phases<sup>7</sup>. Then an additional coupling leads to a constant Zeeman splitting  $g\mu_B B\hat{\sigma}_z$ , where  $g$  is the Landé factor,  $\mu_B$  is the Bohr magneton and  $\hat{\sigma}_z$  is the Pauli matrix acting on the spins. The tight-binding Hamiltonian of interest for our work

then takes the following form

$$\mathcal{H} = t \sum_{\langle k,l \rangle} e^{i\phi_{lk}} c_k^\dagger c_l + i\lambda_{\text{SO}} \sum_{\langle\langle k,l \rangle\rangle} \nu_{k,l} e^{i\phi_{lk}} c_k^\dagger \hat{\sigma}_z c_l + i\lambda_{\text{R}} \sum_{\langle k,l \rangle} e^{i\phi_{lk}} c_k^\dagger (\hat{\boldsymbol{\sigma}} \times \mathbf{d}_{kl})_z c_l + 2\pi\Phi\lambda_{\text{Z}} \sum_k c_k^\dagger \hat{\sigma}_z c_k. \quad (1)$$

Here,  $c_k^{(\dagger)} = (c_{k,\uparrow}, c_{k,\downarrow})^{(\dagger)}$  are the annihilation (creation) operators on the lattice site  $k$  for fermions with spin components up and down. The first two terms in Eq. (1) correspond, respectively to NN and NNN hopping on the honeycomb lattice, with the associated amplitudes  $t$  and  $\lambda_{\text{SO}}$ . The second term is due to the ISO coupling and is characterized by spin-dependent amplitudes, with  $\nu_{kl} = \pm 1$  according to the orientation of the path connecting the NNN sites  $k$  and  $l$ . The Peierls phases,  $\phi_{lk} = i \int_l^k \mathbf{A} \cdot \mathbf{dl}$ , act on both the NN and NNN hopping terms and have been obtained in Ref. 8 using the Landau gauge  $\mathbf{A} = (0, Bx, 0)$ . Here, we set  $\hbar = e = 1$  and we use the hopping parameter  $t$  and the bond length  $a \equiv 1$  as the energy and length units, respectively. The Peierls phases are generally expressed in terms of the dimensionless parameter  $\Phi = S_6 B / 2\pi$ , which represents the number of magnetic flux quanta per plaquette, where  $S_6 = 3\sqrt{3}/2$  is the area of the plaquette. The third term corresponds to a Rashba SO coupling, which acts as a spin mixing perturbation between NN sites. In this term,  $\lambda_{\text{R}}$  is the coupling strength,  $\hat{\boldsymbol{\sigma}}$  is the vector of Pauli matrices and  $\mathbf{d}_{kl}$  is the vector between sites  $k$  and  $l$ . The last term in Eq. (1) is the constant Zeeman splitting, where we set  $\lambda_{\text{Z}} = g\mu_B S_6^{-1}$ . At this point, let us comment on the order of the different parameters for realistic condensed-matter physics experiments. For graphene, the hopping, ISO, and Zeeman parameters are in the order of  $t \sim 1$  eV,  $\lambda_{\text{SO}} \sim 10^{-5}t$  and  $\lambda_{\text{Z}} \sim 0.1t$ . Therefore, the ISO coupling is negligible, whereas for reasonable magnetic field strengths  $B \sim 10$  T, corresponding to  $\Phi \sim 10^{-4}$ , the Zeeman splitting is small, but observable<sup>9</sup>. The recently discovered topological insulators HgTe and Bi-based compounds exhibit large spin-orbit coupling and Landé  $g$ -factor, and are thus good candidates for the observation of the topological phases discussed here<sup>10-12</sup>.

Alternatively, the potential realization of the model (1) with ultra-cold atoms trapped in optical lattices allows us to envisage the interesting case of extremely large magnetic fluxes  $\Phi \sim 0.1 - 1$ , where the spectral gaps  $\Delta \sim 0.1 - 1t$  lead to Hofstadter fractal structures<sup>7</sup>. In this high-flux regime, and for standard values of the other parameters (cf. above), the Zeeman splitting generally dominates  $2\pi\Phi\lambda_{\text{Z}} \gg \lambda_{\text{SO}}$  and one can often neglect the effect of SO coupling in Eq. (1). In this scenario, the interplay between the magnetic field and the spin-orbit interaction only occurs in the range  $0 < \Phi < 0.1$ , where the spectral gaps are unfortunately small compared to the temperatures reached in cold-atom laboratories. However, in contrast to condensed-matter experiments (in which  $\lambda_{\text{Z}}$  is basically fixed by the Landé factor  $g$ ), optical lattice setups allow us to tune every parameter individually

to arbitrary values. In this framework, exotic configurations could be realized, e.g., featuring large magnetic flux and spin-orbit couplings while keeping the Zeeman splitting *low*. Furthermore, the non-interacting limit can be easily reached through Feshbach resonances. In the following Sections, we demonstrate the existence of robust new topological phases which could be engineered in the high-flux regime, by appropriately tuning the Zeeman splitting and the SO terms. We then comment on the possible realizations of this model, in condensed-matter and cold-atom laboratories, and discuss the implications of our findings.

Although our calculations were performed for the honeycomb lattice, our predictions do not rely on this specific geometry: Any Dirac system exhibiting large Zeeman splitting and spin-orbit interactions will exhibit a similar behavior. In particular, Dirac cones were shown to emerge in HgTe and Bi-based compounds<sup>12</sup>, as well as in square optical lattices subjected to staggered<sup>13,14</sup> or non-Abelian<sup>15</sup> gauge fields.

## II. RESULTS

Topological phases are distinguished by the unusual quantum currents carried by gapless edge states. The non-trivial properties associated with these current-carrying states are obtained by computing the energy spectrum  $E = E(k)$  on a cylindrical geometry<sup>16</sup>. One then typically encounters a few gapless states inside the bulk energy gaps, which are localized at the edges. Furthermore, the direction of the edge current can be determined from the slope  $\partial E/\partial k$ . The transport coefficients are equally evaluated through the computation of the topological invariants, which are associated with the bulk energy bands (see Methods). The spectrum and its corresponding topological phases have been widely studied for the spinless case  $\lambda_R = \lambda_{SO} = \lambda_Z = 0$ , where a finite magnetic flux  $\Phi$  leads to a peculiar QH effect<sup>17</sup>. In the other limit, where  $\Phi = 0$ , a finite ISO strength  $\lambda_{SO}$  is known to open a QSH gap of magnitude  $\Delta = 6\sqrt{3}\lambda_{SO}$ <sup>4,5</sup>. In both these limits, the presence of chiral or helical edge states can be investigated by solving Eq. (1) on an abstract cylindrical geometry, namely by considering open boundary conditions along the  $x$  direction. We note that the dispersion relations  $E = E(k)$  obtained from the cylindrical geometry depend on the edges considered for the computations (i.e. zigzag, armchair or bearded). Obviously, this choice does not modify the physical properties discussed here, as they rely on topological properties characterizing the bulk states. Finally, let us comment on the fact that the topological transport of realistic finite systems can be obtained through the edge-state analysis, by focusing on a single edge of the abstract cylinder.

### A. The weak QSH phase, the spin-filtered and the spin-imbalanced topological phases

Let us first discuss the fate of the QSH phase as a uniform magnetic field is progressively increased in a realistic condensed-matter framework. The main effect of this additional field is to break time-reversal symmetry and therefore to allow scattering processes between the counter-propagating edge states characterizing the QSH phase<sup>4,5</sup> (cf. Fig. 1 (b)). Therefore, although the bulk energy gap and the non-trivial topological index associated with the QSH phase at half-filling are preserved for a finite magnetic flux, the time-reversal violation *weakens* the topological phase in the presence of disorder. In the following, we will refer to such phases as “weak QSH phases”. Note however that such phases would still be robust in optical lattices, where disorder is absent. Besides, the magnetic field creates spin-degenerate QH phases away from half-filling. For sufficiently large magnetic fields, the weak-QSH gap at half-filling is destroyed (e.g., when  $\lambda_{SO} = 0.05t$  and  $\lambda_Z = 0.1t$ , this gap closing occurs at  $\Phi \approx 0.14$ ) and only the standard QH gaps remain.

Let us investigate an alternative scenario, starting from spin-degenerate QH phases in the absence of Zeeman splitting and spin-orbit coupling. We base the following discussion on the situation in which  $\Phi = 1/3$  and where all the other parameters can be tuned individually, such as in optical lattice experiments. The conclusions hold for arbitrary large flux but several effects could be probed in condensed-matter experiments as well, where the flux per plaquette cannot be very large, due to the typically small values of the lattice constant (cf. Discussions). The energy spectrum for  $\Phi = 1/3$  is exhibited in Fig. 2 (a), which shows four spin-degenerate QH phases with the Hall conductivity  $\sigma_H = \pm 2$  in units of the conductivity quantum. Now, let us turn on the Zeeman splitting. The effect of the Zeeman splitting is two-fold: by lifting the spin-degeneracy, the Zeeman term separates the QH phases and eventually generates *spin-filtered* QH phases (cf. Fig. 1 (a) and Fig. 2 (b)). Besides, the Zeeman term creates a weak QSH phase at half-filling. It is remarkable that such a QSH phase is produced in the absence of ISO coupling, which highlights the great similarity between the Zeeman and the ISO terms<sup>18</sup> in Eq. (1). However, this “Zeeman” QSH phase is weak because of the time-reversal violation, as already discussed above. Starting from this configuration, we progressively add the ISO coupling. As shown in Fig. 3 (a), the ISO opens new gaps in the energy spectrum, the topological character of which highly depends on the Zeeman splitting. For  $\lambda_Z = 0.5t$  and  $\lambda_{SO} = 0.35t$ , a weak QSH gap opens at  $E \approx 1.1t$  (cf. Fig. 3 (a)). Increasing the ISO term further leads to a gap closing (cf. Fig. 3 (b)) and eventually to an unexpected topological phase transition. As represented in Fig. 3 (c), the gap is now characterized by a strong *spin-imbalanced* quantum Hall phase (cf. Fig. 1 (d)). Indeed, each edge is populated by chiral edge states with

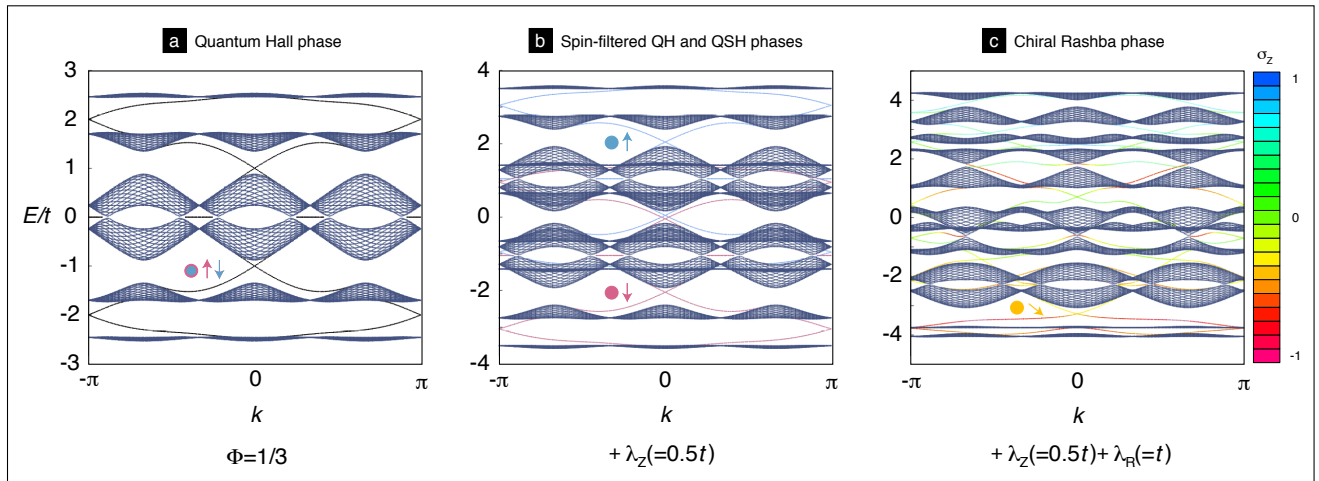


FIG. 2: **Generating a chiral Rashba phase on the edges:** The energy spectrum  $E = E(k)$  is represented as a function of the momentum, in a cylindrical geometry with zigzag edges. **(a)** Several QH phases are generated by a magnetic flux  $\Phi = 1/3$ . When the Fermi energy lies in the gap at  $E \approx -t$ , a single spin-degenerate edge state propagates on each edge. **(b)** The inclusion of the Zeeman splitting lifts the spin degeneracy and creates spin-filtered QH phases at  $E = \pm 2.25t$  and  $E = \pm 3t$ . At half-filling, the Zeeman splitting opens a “weak” QSH gap. **(c)** The addition of the Rashba term then allows for flipping the spin of the edge state to an arbitrary orientation. When the Fermi energy  $E_F \approx -3.25t$ , the single edge state has spin components  $\sigma_z \approx -0.5$  and  $\sigma_\perp \approx 0.5$  (cf. orange dot). Here, the bulk energy bands are depicted in dark blue.

different spin components and  $N_\uparrow = 1 \neq N_\downarrow = 2$ . In this configuration, when the Fermi energy  $E_F$  lies in the gap at  $E \approx 1.3t$ , the Hall conductivity and the spin-Hall conductivity differ, since  $\sigma_H = 3$  and  $\sigma_H^s = -1$  in units of charge and spin conductivities, respectively. Note that the chiral character of these polarized current-carrying edge states guarantees the robustness of this remarkable quantum phase against external perturbations. In this sense, the SO coupling has driven a transition from a *weak* QSH to a *strong spin-imbalanced* topological phase.

Consequently, by adjusting the Zeeman splitting and the ISO coupling, one is able to control the spin texture associated with the chiral edge states of topological insulators. It is interesting to observe that a large Zeeman splitting (i.e., large  $g$  factor) would already produce chiral spin-filtered edge states, where spins of the same nature carry both charge and spin currents. In such a configuration, and when the Fermi energy is located inside a spin-filtered QH bulk gap, a two-component Fermi gas will exhibit edge currents transported by a single species only. Moreover, the addition of the ISO coupling allows for the attractive possibility to engineer robust polarized spin currents, for which the spin-imbalance  $N_\uparrow \neq N_\downarrow$  can be tuned.

## B. The Chiral Rashba phase

The Rashba SO coupling has dramatic consequences on the system described by Eq. (1), as it induces spin mixing. In the presence of a magnetic field, the Rashba term lifts the degeneracy of the original QH phases and eventually opens new topologically *trivial* gaps.

Interestingly, the Rashba term therefore *destroys* the topological nature of the QH gaps in certain regions of the spectrum. In addition, the Rashba coupling partially polarizes the edge currents associated with the QH phases.

A remarkable spin-manipulation process can be envisaged by combining the effects of the Rashba spin-mixing perturbation and the Zeeman splitting. As already mentioned above, the Zeeman splitting generates spin-filtered edge states in the QH gaps. In the example illustrated in Fig. 2 (b), a single spin-down particle propagates along the edge of the sample when  $E_F \approx -2.25t$ , for  $\Phi = 1/3$  and  $\lambda_Z = 0.5t$ . As shown in Fig. 2 (c), one can then progressively increase the Rashba coupling, and control the spin orientation of this specific and *unique* chiral edge state. This process indeed modifies the band structure, as well as the spin textures associated with the edge current, leading to the chiral Rashba phase illustrated in Fig. 1 (c): the spin components of this single edge state are now  $\sigma_z = -0.5$  and  $\sigma_\perp = 0.5$ , where  $\sigma_\perp$  is the spin component in the direction perpendicular to both the direction of propagation and the applied magnetic field. For  $\lambda_R = t$ , this single edge state can be reached by adjusting the Fermi energy to the value  $E_F \approx -3.25t$ . Note that the Rashba term tends to close the gap and to cant the edge-state spin, whereas the Zeeman term tends to open the gap and to align the spin along the vertical. Finally, let us mention that the combination of Zeeman splitting, Rashba SO coupling and  $s$ -wave superconductivity would lead to a topological superconductor exhibiting Majorana fermions<sup>19</sup>.

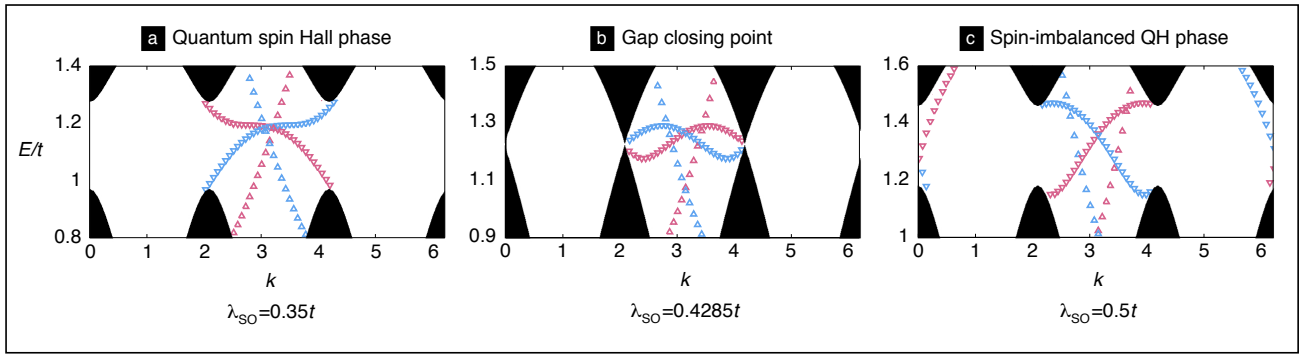


FIG. 3: **Phase transition from the QSH to the spin-imbalanced QH phase:** The energy spectrum  $E = E(k)$  is represented as a function of the momentum, in a cylindrical geometry with bearded edges. Here we set  $\Phi = 1/3$  and  $\lambda_z = 0.5t$ . Spin up [resp. down] states are represented by up [resp. down] triangles and the two colors designate the two edges of the cylinder where the states are localized. **(a)** The weak QSH phase is characterized by counter-propagating spins with opposite sign. **(b)** The gap closes for  $\lambda_{SO} \approx 0.4285t$ . **(c)** The spin-imbalanced QH phase: each edge features one spin-up and two spin-down states propagating in the *same* direction. Here, the bulk bands are depicted in black.

### III. DISCUSSIONS

The experimental realization of the novel topological phases presented here constitutes an appealing target for both condensed-matter and cold-atom laboratories. In principle, one could realize the model described by Eq. (1) by trapping ultracold fermions in optical lattices. This set-up has the advantage of allowing us to explore a wide range of the parameters space associated with the model. The honeycomb geometry considered in this work has already been realized experimentally<sup>20</sup>, but alternative geometries with additional pseudo-spin degrees of freedom could lead to similar effects<sup>13–15</sup>. The main elements that have to be added to these lattice systems are the spin-orbit couplings and a uniform magnetic field. Both effects have already been engineered in cold gases confined to a single trap, by using Raman transitions between internal atomic states<sup>21–23</sup>. In this framework, they are generally referred to as non-Abelian and Abelian synthetic gauge fields. However, different methods are required for generating such fields in atomic *lattices*. Although they have not yet been experimentally realized, several routes have already been suggested in Refs. 15,24–28. These proposals could be adjusted to generate the Rashba and ISO terms, as well as the Peierls phases, in a honeycomb optical lattice. Moreover, the Zeeman splitting in Eq. (1) could be easily produced by static magnetic fields. Nowadays, the main difficulty encountered by cold-atom experimentalists to realize topological insulating phases is the detection of the gapless edge states, since standard confining traps will generally alter the bulk bands and destroy the edge-state structures<sup>29</sup>. To overcome this drawback, it is possible to either design sharp walls (e.g. using Laguerre-Gaussian traps) or to create interfaces in the system (e.g. inducing hopping anisotropy by abruptly changing the intensity of the Raman coupling within the trap<sup>27</sup>). We would like to stress

that the topological phases presented in Figs. 2 and 3 are protected by bulk energy gaps  $\Delta \sim 0.1 - 1t$ , thus requiring achievable temperatures  $T \sim 10$  nK for their observation. Finally, let us comment on the fact that spin-imbalanced atomic gases have recently been under intense investigations<sup>30</sup>. In one-dimensional optical lattices, such phases lead to the realization of exotic pairing mechanisms<sup>31</sup> and share fascinating similarities with the quark-gluon plasma<sup>32</sup>. Surprisingly, our 2D model features spin-imbalanced (edge) states that are confined to the 1D edge of the system, but also possess a chiral nature. The interplay between spin-imbalance, chirality and controllable interactions should certainly lead to rich physics not envisaged so far.

On the other hand, the new topological phases reported in this work could also be realized in condensed-matter experiments, where extraordinary high magnetic fields, Zeeman splitting and SO coupling have recently been achieved. In regard to graphene, the hope to observe topological spin currents has faded away since the original works by Kane and Mele<sup>4,5</sup>. Indeed, real values of  $\lambda_{SO}$  turned out to be in the range  $0.001 - 0.05$  meV<sup>33</sup>, and are thus too small for observing the topological effects. Interestingly, the Rashba coupling may be controlled by an external electric field, and it has been shown that values as large as  $\lambda_R \approx 0.2$  eV can be experimentally reached by growing epitaxial graphene on top of a Ni(111) substrate<sup>34</sup>. Moreover, it was found that high values of the Rashba SO coupling (accompanied by the spin re-orientation at the edges) may also be induced by curving nanoribbons<sup>35</sup>. Besides the large Rashba coupling, gigantic pseudo-magnetic fields, greater than 300 T, have been recently realized in strain-induced graphene nanobubbles<sup>36</sup>. Here, we have shown that the presence of the Zeeman splitting term significantly increases the size of the gaps, thus rendering new effects such as spin-imbalanced phases more robust and easier to observe. At fields of about 30 T, the Zeeman gaps are

in the order of  $100\text{ K}^9$ , while the quantum Hall gaps are much larger than the room temperature<sup>37</sup>. Thus, the realization of Zeeman-induced topological phases remains elusive in graphene, but should not be definitively ruled out. We note that honeycomb arrays of quantum dots are currently in development and will constitute interesting alternatives for the exploration of topological phases in the high-flux regime, due to their large lattice constant<sup>38</sup>.

The QSH effect has nevertheless been observed in other 2D compounds that have considerably larger values of  $\lambda_{\text{SO}}$ , such as Hg(Cd)Te quantum wells<sup>10</sup>, for which gaps in the order of  $10\text{ meV}$  have been reported<sup>39,40</sup>. In addition, in the 2D HgTe material the  $g$ -factor can be very large (i.e.  $g = 55$ ) and spin-resolved quantum Hall states have already been observed at low fields<sup>41</sup>. Right after the discovery of the QSH effect in the 2D HgTe compound, topological insulating states were observed in the 3D materials  $\text{Bi}_{1-x}\text{Sb}_x$ ,  $\text{Bi}_2\text{Se}_3$ , and  $\text{Bi}_2\text{Te}_3$ <sup>12</sup>. Since then, the field has evolved remarkably fast, topological insulators have been classified according to their mathematical properties<sup>42</sup> and several new materials (e.g. Heusler compounds<sup>43</sup> and pyrochlore iridates<sup>44</sup>) are being studied. Moreover, the competition between the Rashba SO and the Zeeman splitting term is being currently experimentally investigated by Ong *et al.* in the  $\text{Bi}_2\text{Te}_2\text{Se}$  compound<sup>45</sup>. This 3D material has a large  $g$ -factor, which ranges from 25-30 and a reduced bulk conductivity, which allows for the observation of surface effects. In the presence of a perpendicular magnetic field, Shubnikov-de Haas quantum oscillations were observed up to  $35\text{ T}$ <sup>46</sup>. We expect that the chiral spin polarized currents proposed here, with the spin pointing in a direction that may solely be determined by the Rashba interaction strength, could be experimentally observed with this setup.

Finally, it remains to emphasize that the semiclassical analogues of the effects described here have already been experimentally realized<sup>47</sup>. Indeed, spin manipulation in a ferromagnet-semimetal-ferromagnet heterostructure is at the core of the Datta-Das transistor operation<sup>6</sup>. If the semimetal between the two ferromagnets with inverted polarization is able to rotate the spin of the injected spin

polarized electron, the current can propagate, otherwise not<sup>48</sup>. Here we show that for materials where the Rashba and Zeeman effects are large enough, a “quantized” version of this phenomenon might occur. In addition, imbalanced spin currents, with  $N_{\uparrow} > N_{\downarrow}$ , e.g., are also realized in spintronics<sup>47</sup>. Our calculations show that the “quantized” version of this effect may also be in reach with the state-of-the-art experimental techniques, thus paving the way to the realization of quantum spin-valves and quantum spin-injected field-effect transistors, which may have a substantial impact on future nanotechnology.

#### IV. METHODS

In this work, we solve the spin-1/2 graphene model of Refs. 4,5 in the presence of a uniform magnetic field and spin-orbit interactions. Here, both the Rashba and the intrinsic SO terms are considered and each of them leads to radically different effects. The staggered potential introduced in Refs. 4,5, driving transitions between trivial and non-trivial topological insulating phases, is omitted in this work for the sake of simplicity. We also neglect the effects of interactions between the particles. This non-interacting limit can be easily reached at low densities or, for cold-atom realizations, using Feshbach resonances. The key ingredient of our original study is the uniform magnetic field  $\mathbf{B} = B\mathbf{1}_z$ , which modifies the Kane and Mele model in two ways: the magnetic field enters the model through the so-called Peierls phases<sup>7</sup>, and additionally leads to a constant Zeeman splitting  $g\mu_B B\hat{\sigma}_z$ . The resulting tight-binding Hamiltonian is explicitly given in Eq. (1).

Since the honeycomb lattice has two sites per unit cell, the single-particle wave function can be written as  $\Psi(n, m) = (\psi_A(n, m), \psi_B(n, m))$ , where  $(n, m)$  are integers labeling the unit cells<sup>8</sup>. In this notation, the spin indices ( $\sigma = \uparrow, \downarrow$ ) are omitted. Using the Landau gauge for the uniform magnetic field, we can set  $\Psi(n, m) = \exp(ikm)\Psi(n)$  and the single-particle Schrödinger equation then takes the form of a generalized Harper equation

$$\begin{aligned}
 E\Psi(n) &= \mathcal{D}(n)\Psi(n) + \mathcal{R}(n)\Psi(n+1) + \mathcal{R}^\dagger(n-1)\Psi(n-1), \\
 \mathcal{D}(n) &= \begin{pmatrix} 2\lambda_{\text{SO}}\hat{\sigma}_z \sin(2\pi\Phi(n + \frac{1}{6}) + k) + 2\pi\Phi\lambda_Z\hat{\sigma}_z & t\hat{1} - i\lambda_{\text{R}}\hat{\sigma}_y \\ t\hat{1} + i\lambda_{\text{R}}\hat{\sigma}_y & -2\lambda_{\text{SO}}\hat{\sigma}_z \sin(2\pi\Phi(n + \frac{1}{6}) + k) + 2\pi\Phi\lambda_Z\hat{\sigma}_z \end{pmatrix}, \\
 \mathcal{R}(n) &= \begin{pmatrix} i\lambda_{\text{SO}}\hat{\sigma}_z(g(n+1) - g^*(n+1)e^{-ik}) & 0 \\ f(n+1)(t\hat{1} - i\lambda_{\text{R}}\hat{\gamma}_-) + f^*(n+1)e^{-ik}(t\hat{1} - i\lambda_{\text{R}}\hat{\gamma}_+) & -i\lambda_{\text{SO}}\hat{\sigma}_z(h(n+1) - h^*(n+1)e^{-ik}) \end{pmatrix}, \quad (2)
 \end{aligned}$$

where  $f(n) = \exp(i\pi\Phi n)$ ,  $g(n) = \exp(i\pi\Phi(n - 1/3))$ ,  $h(n) = \exp(i2\pi\Phi(n + 1/6))$  and  $\hat{\gamma}_{\pm} = \pm\frac{\sqrt{3}}{2}\hat{\sigma}_x + \frac{1}{2}\hat{\sigma}_y$ . The Peierls phases are expressed in terms of the dimensionless parameter  $\Phi = S_6 B/2\pi$ , which represents the number of magnetic flux quanta per plaquette with area  $S_6 = 3\sqrt{3}/2$ .

sionless parameter  $\Phi = S_6 B/2\pi$ , which represents the number of magnetic flux quanta per plaquette with area  $S_6 = 3\sqrt{3}/2$ .

For rational fluxes  $\Phi = p/q$ , where  $p$  and  $q$  are integers, the system is periodic with period  $2q$  along the  $n$  direction (note that this periodicity property depends on the gauge used). Therefore, the bulk energy spectrum can be obtained by imposing periodic boundary conditions along this direction and by diagonalizing the corresponding  $8q \times 8q$  Hamiltonian matrix. Solving Eq. (2) on this torus geometry further allows us to compute the Chern numbers  $N_{\text{ch}}$ , which are topological integers characterizing the bulk bands<sup>49</sup>. Considering twisted-periodic boundary conditions, one can also compute the  $\mathbb{Z}_2$  topological index through its related spin-Chern number<sup>50–52</sup>. The numerical evaluation of the Chern [resp. spin-Chern] numbers yield the Hall charge [resp. spin] conductivities, hence indicating the presence of non-trivial topological phases as a function of the Fermi energy.

In the absence of the spin-mixing Rashba term, the dimensionless Hall conductivity equals  $\sigma_H = (N_{\uparrow} + N_{\downarrow})$ , and results from  $|N_{\uparrow}|$  spin-up and  $|N_{\downarrow}|$  spin-down current-carrying edge states. Here, the quantities  $N_{\uparrow, \downarrow}$  are integers, the sign of which is given by the orientation of the corresponding edge states. The dimensionless spin Hall conductivity is then given by the difference  $\sigma_H^s = (N_{\uparrow} - N_{\downarrow})$ . The number of gapless edge states  $|N_{\uparrow, \downarrow}|$  and their orientation can be equally evaluated by computing the bulk topological indices, or by solving Eq. (2) on a finite (cylindrical) geometry<sup>16</sup>.

The standard (spin-degenerate) QH phase corresponds to  $\sigma_H = \nu$  and  $\sigma_H^s = 0$ , where  $\nu$  is an integer. The filtered QH phase (cf. Fig. 1 (a)) corresponds to  $|\sigma_H^s| = |\sigma_H|$ , while the QSH phase (cf. Fig. 1 (b)) is characterized by  $\sigma_H^s = \pm 2 \bmod 4$  and  $\sigma_H = 0$ . In the two latter cases, the spin conductivity is quantized in the absence of spin-mixing and is given by  $\sigma_H^s \times (e/4\pi)$ <sup>53</sup>. A spin-imbalanced

QH phase (cf. Fig. 1 (d)) is identified when both spin and charge conductivities are non-vanishing *and*  $|\sigma_H^s| \neq |\sigma_H|$ : the spin and charge transport differ, i.e.,  $N_{\uparrow}$  and  $N_{\downarrow}$  are unequal and nonzero. All these phases are robust against disorder in the presence of the magnetic field as long as they feature chiral edge states, namely when all the edge states contributing to the current have the same orientation:  $\text{sign}(N_{\uparrow}) = \text{sign}(N_{\downarrow})$ . We stress that non-chiral spin-imbalanced phases are pervasive in our model and that these weak topological phases could also be detected in the absence of disorder.

The Rashba SO term changes the spin orientation of spin-filtered chiral edge states, which can be isolated by a large Zeeman splitting (cf. Fig. 2). The spin orientation of these states can be evaluated by computing the expectation values

$$\langle \sigma_{\mu} \rangle = \langle \Psi | \hat{\sigma}_{\mu} | \Psi \rangle = \sum_n \Psi^{\dagger}(n) (\hat{1} \otimes \hat{\sigma}_{\mu}) \Psi(n) \quad (3)$$

of the spin components, where  $\hat{1}$  is the identity matrix acting on the lattice pseudospin ( $A, B$ ) space and  $\mu = x, y, z$ .

### Acknowledgments

NG thanks the F.R.S-F.N.R.S (Belgium) for financial support. WB and CMS thank the Netherlands Organisation for Scientific Research (NWO) for financial support. The authors acknowledge A. Bermudez, N. P. Ong, I. B. Spielman, F. Gerbier, J. Dalibard and M. Lewenstein for inspiring discussions. Correspondence and requests for materials should be addressed to N. G.

\* Electronic address: [ngoldman@Tulb.ac.be](mailto:ngoldman@Tulb.ac.be)

<sup>1</sup> von Klitzing, K. The quantized Hall effect. *Rev. Mod. Phys.* **58**, 519–531 (1986).

<sup>2</sup> Thouless, D. J., Kohmoto, M., Nightingale, M. P. & den Nijs, M. Quantized Hall conductance in a two-dimensional periodic potential. *Phys. Rev. Lett.* **49**, 405–408 (1982).

<sup>3</sup> Kohmoto, M. Topological invariant and the quantization of the Hall conductance. *Ann. Phys.* **160**, 343–354 (1985).

<sup>4</sup> Kane, C. L. & Mele, E. J.  $\mathbb{Z}_2$  topological order and the quantum spin Hall effect. *Phys. Rev. Lett.* **95**, 146802 (2005).

<sup>5</sup> Kane, C. L. & Mele, E. J. Quantum spin Hall effect in graphene. *Phys. Rev. Lett.* **95**, 226801 (2005).

<sup>6</sup> Datta, S. & Das, B. Electronic analog of the electro-optic modulator. *Appl. Phys. Lett.* **56**, 665–667 (1990).

<sup>7</sup> Hofstadter, D. R. Energy levels and wave functions of Bloch electrons in rational and irrational magnetic fields. *Phys. Rev. B* **14**, 2239–2249 (1976).

<sup>8</sup> Hou, J.-M. & Yang, W.-X. Next-nearest-neighbor-tunneling-induced symmetry breaking of Hofstadter’s butterfly spectrum for ultracold atoms on the honeycomb lattice. *Phys. Lett. A* **373**, 2774–2777 (2009).

<sup>9</sup> Abanin, D. A., Lee, P. A. & Levitov, S. Spin-Filtered Edge States and Quantum Hall Effect in Graphene. *Phys. Rev. Lett.* **96**, 176803 (2006).

<sup>10</sup> König, M. *et al.* Quantum spin Hall insulator state in HgTe quantum wells. *Science* **318**, 766–770 (2007).

<sup>11</sup> Roth, A. *et al.* Nonlocal transport in the quantum spin Hall state. *Science* **325**, 294–297 (2009).

<sup>12</sup> Hasan, M. Z. & Kane, C. L. Colloquium: Topological insulators. *Rev. Mod. Phys.* **82**, 3045–3067 (2010).

<sup>13</sup> Lim, L.-K., Morais Smith, C. & Hemmerich, A. Staggered-vortex superfluid of ultracold bosons in an optical lattice. *Phys. Rev. Lett.* **100**, 130402 (2008).

<sup>14</sup> Lim, L.-K., Hemmerich, A. & Morais Smith, C. Artificial staggered magnetic field for ultracold atoms in optical lattices. *Phys. Rev. A* **81**, 023404 (2010).

<sup>15</sup> Goldman, N. *et al.* Non-Abelian optical lattices: Anomalous quantum Hall effect and Dirac fermions. *Phys. Rev. Lett.* **103**, 035301 (2009).

<sup>16</sup> Hatsugai, Y. Edge states in the integer quantum Hall effect and the Riemann surface of the Bloch function. *Phys. Rev. B* **48**, 11851–11862 (1993).

<sup>17</sup> Hatsugai, Y., Fukui, T. & Aoki, H. Topological analysis

- of the quantum Hall effect in graphene: Dirac-Fermi transition across van Hove singularities and edge versus bulk quantum numbers. *Phys. Rev. B* **74**, 205414 (2006).
- <sup>18</sup> Abanin, D. A., Gorbachev, R. V., Novoselov, K. S., Geim, A. K. & Levitov, L. S. Giant spin-Hall effect induced by Zeeman interaction in graphene (2011). arXiv:1103.4742.
- <sup>19</sup> Sau, J. D., Sensarma, R., Powell, S., Spielman, I. B. & Das Sarma, S. Chiral Rashba spin textures in ultra-cold Fermi gases (2010). arXiv:1012.3170.
- <sup>20</sup> Soltan-Panahi, P. *et al.* Multi-component quantum gases in spin-dependent hexagonal lattices. *Nature Phys.* (DOI: 10.1038/nphys1916) (2011).
- <sup>21</sup> Lin, Y.-J., Compton, R. L., Jiménez-García, K., Porto, J. V. & Spielman, I. B. Synthetic magnetic fields for ultracold neutral atoms. *Nature* **462**, 628–632 (2009).
- <sup>22</sup> Lin, Y.-J., Jiménez-García, K. & Spielman, I. B. Spin-orbit-coupled Bose-Einstein condensates. *Nature* **471**, 83–86 (2011).
- <sup>23</sup> Dalibard, J., Gerbier, F., Juzeliūnas, G. & Öhberg, P. Artificial gauge potentials for neutral atoms (2010). arXiv:1008.5378.
- <sup>24</sup> Jaksch, D. & Zoller, P. Creation of effective magnetic fields in optical lattices: the Hofstadter butterfly for cold neutral atoms. *New J. Phys.* **5**, 56 (2003).
- <sup>25</sup> Osterloh, K., Baig, M., Santos, L., Zoller, P. & Lewenstein, M. Cold atoms in non-Abelian gauge potentials: From the Hofstadter “moth” to lattice gauge theory. *Phys. Rev. Lett.* **95**, 010403 (2005).
- <sup>26</sup> Gerbier, F. & Dalibard, J. Gauge fields for ultracold atoms in optical superlattices. *New J. Phys.* **12**, 033007 (2010).
- <sup>27</sup> Goldman, N. *et al.* Realistic time-reversal invariant topological insulators with neutral atoms. *Phys. Rev. Lett.* **105**, 255302 (2010).
- <sup>28</sup> Bermudez, A. *et al.* Wilson Fermions and Axion Electrodynamics in Optical Lattices. *Phys. Rev. Lett.* **105**, 190404 (2010).
- <sup>29</sup> Stanescu, T. D., Galitski, V. & Das Sarma, S. Topological states in two-dimensional optical lattices. *Phys. Rev. A* **82**, 013608 (2010).
- <sup>30</sup> Nascimbène, S. *et al.* Collective oscillations of an imbalanced Fermi gas: Axial compression modes and polaron effective mass. *Phys. Rev. Lett.* **103**, 170402 (2009).
- <sup>31</sup> Liao, Y.-a. *et al.* Spin-imbalance in a one-dimensional Fermi gas. *Nature* **467**, 567–569 (2010).
- <sup>32</sup> Casalbuoni, R. & Nardulli, G. Inhomogeneous superconductivity in condensed matter and QCD. *Rev. Mod. Phys.* **76**, 263–320 (2004).
- <sup>33</sup> Boettger, J. C. & Trickey, S. B. First-principles calculation of the spin-orbit splitting in graphene. *Phys. Rev. B* **75**, 121402 (2007).
- <sup>34</sup> Dedkov, Y. S., Fonin, M., Rüdiger, U. & Laubschat, C. Rashba effect in the graphene/Ni(111) system. *Phys. Rev. Lett.* **100**, 107602 (2008).
- <sup>35</sup> Gosálbez-Martínez, D., Palacios, J. J. & Fernández-Rossier, J. Spin-orbit interaction in curved graphene ribbons. *Phys. Rev. B* **83**, 115436 (2011).
- <sup>36</sup> Levy, N. *et al.* Strain-induced pseudo-magnetic fields greater than 300 Tesla in graphene nanobubbles. *Science* **329**, 544–547 (2010).
- <sup>37</sup> Novoselov, K. S. *et al.* Room-temperature quantum Hall effect in graphene. *Science* **315**, 1379 (2007).
- <sup>38</sup> De Simoni, G. *et al.* Delocalized-localized transition in a semiconductor two-dimensional honeycomb lattice. *Appl. Phys. Lett.* **97**, 132113 (2010).
- <sup>39</sup> Brüne, C. *et al.* Quantum Hall effect from the topological surface states of strained bulk HgTe (2011). arXiv:1101.2627.
- <sup>40</sup> Novik, E. G. *et al.* Band structure of semimagnetic  $\text{Hg}_{1-y}\text{Mn}_y\text{Te}$  quantum wells. *Phys. Rev. B* **72**, 035321 (2005).
- <sup>41</sup> Büttner, B. *et al.* Single valley Dirac fermions in zero-gap HgTe quantum wells. *Nature Phys.* (DOI: 10.1038/nphys1914) (2011). Advance online publication.
- <sup>42</sup> Ryu, S., Schnyder, A. P., Furusaki, A. & Ludwig, A. W. W. Topological insulators and superconductors: tenfold way and dimensional hierarchy. *New J. Phys.* **12**, 065010 (2010).
- <sup>43</sup> Zhang, H.-J. *et al.* Topological insulators in ternary compounds with a honeycomb lattice (2010). arXiv:1010.2195.
- <sup>44</sup> Wan, X., Vishwanath, A. & Savrasov, S. Y. Computational design of axion insulators based on 5d spinels compounds (2011). arXiv:1103.4634.
- <sup>45</sup> Ong, N. P. (2011). Presentation at APS March Meeting.
- <sup>46</sup> Xiong, J., Petersen, A. C., Qu, D., Cava, R. & Ong, N. P. Quantum oscillations in a topological insulator  $\text{Bi}_2\text{Te}_2\text{Se}$  with large bulk resistivity ( $6 \Omega\text{cm}$ ) (2011). arXiv:1101.1315.
- <sup>47</sup> Wolf, S. A. *et al.* Spintronics: A spin-based electronics vision for the future. *Science* **294**, 1488–1495 (2001).
- <sup>48</sup> Koo, H. C. *et al.* Control of spin precession in a spin-injected field effect transistor. *Science* **325**, 1515–1518 (2009).
- <sup>49</sup> Fukui, T., Hatsugai, Y. & Suzuki, H. Chern numbers in discretized Brillouin zone: Efficient method of computing (spin) Hall conductances. *J. Phys. Soc. Jpn* **74**, 1674–1677 (2005).
- <sup>50</sup> Sheng, D. N., Weng, Z. Y., Sheng, L. & Haldane, F. D. M. Quantum spin-Hall effect and topologically invariant Chern numbers. *Phys. Rev. Lett.* **97**, 036808 (2006).
- <sup>51</sup> Fukui, T. & Hatsugai, Y. Topological aspects of the quantum spin-Hall effect in graphene:  $Z_2$  topological order and spin Chern number. *Phys. Rev. B* **75**, 121403 (2007).
- <sup>52</sup> Qi, X.-L., Wu, Y.-S. & Zhang, S.-C. General theorem relating the bulk topological number to edge states in two-dimensional insulators. *Phys. Rev. B* **74**, 045125 (2006).
- <sup>53</sup> Bernevig, B. A. & Zhang, S.-C. Quantum spin Hall effect. *Phys. Rev. Lett.* **96**, 106802 (2006).